Eur. Phys. J. C (2023) 83:84
https://doi.org/10.1140/epjc/s10052-022-11164-5

THE EUROPEAN PHYSICAL JOURNAL C

Regular Article - Theoretical Physics

Evolution of scalar field resonances in a braneworld

Qin Tan[1,2], **Yu-Peng Zhang**[1,2], **Wen-Di Guo**[1,2], **Jing Chen**[1,2], **Chun-Chun Zhu**[1,2], **Yu-Xiao Liu**[1,2,a]

[1] Key Laboratory of Theoretical Physics of Gansu Province, Lanzhou Center for Theoretical Physics, School of Physical Science and Technology, Lanzhou University, Lanzhou 730000, China
[2] Institute of Theoretical Physics and Research Center of Gravitation, Lanzhou University, Lanzhou 730000, China

Received: 27 September 2022 / Accepted: 23 December 2022 / Published online: 28 January 2023

Abstract In this work, we investigate the numerical evolution of massive Kaluza–Klein (KK) modes of a scalar field in a thick brane. We derive the Klein–Gordon equation in five-dimensional spacetime, and obtain the evolution equation and the Schrödinger-like equation. With the resonances of the scalar KK modes as the initial data, the scalar field is evolved with the maximally dissipative boundary condition. The results show that there are scalar KK resonant particles with long life on the brane, which indicates that these resonances might be regarded as a candidate for dark matter.

1 Introduction

The nature of dark matter (DM) constitutes one of the most long-standing and puzzling questions in cosmology. There is abundant evidence that nonluminous matter makes up a large fraction of all matter in our universe. Results from cosmological measurements have now determined with exquisite precision the abundance of DM [1]. But the identity of DM remains a mystery. Recently, Barranco et al. proposed that the scalar dynamical resonances could form long-lived configurations around black holes [2–4]. This ultralight scalar resonance might be regarded as a candidate for DM. Such long-lived distribution was then generalized to the Dirac field by Zhou et al. [5]. Since then, these massive dynamical resonances around black holes have garnered much attention [6–15]. The study of resonances of various fields around black holes has stimulated our interest in the evolution of resonances in theories of extra dimensions and braneworld.

The history of extra dimensions and braneworld dates back to the last century. In the 1920s, Kaluza and Klein (KK) proposed a five-dimensional spacetime theory to unify electromagnetic and gravitational interactions [16,17]. Subsequently, extra-dimensional theories remained silent for more than 70 years, until the 1990s when, to solve the huge hierarchy between the Planck and weak scales, some braneworld models were proposed. Two of them have attracted the attention of many researchers. One is the large extra-dimensional model proposed by Arkani-Hamed et al. [18], and the other is the warped extra-dimensional model proposed by Randall and Sundrum [19]. The size of the extra dimensions is finite in these braneworld models. Subsequently, Antoniadis et al. embedded the braneworld model with large extra dimensions into string theory [20]. A notable development was attained in Ref. [21], which showed that even the extra dimension is infinite, and four-dimensional gravity can also be recovered on the brane. Since then, extra-dimensional theories have attracted considerable attention [22–44].

In this paper, we focus on the evolution of the scalar KK resonances on the thick brane, which is generated dynamically by a background scalar field. In a braneworld model, to recover the physics in our four-dimensional spacetime, the zero modes of various fields should be localized on the brane. But in addition to zero modes, there are massive KK modes which might propagate into extra dimensions. KK resonances are a specific class of massive KK modes in braneworld models. Usually, for a volcano-like potential, although massive KK modes cannot be localized on the brane, KK resonances can be quasi-localized [45]. Previous studies have investigated resonances of various fields on thick branes [45–55]. To the best of our knowledge, no studies to date have explored the evolution of KK resonances of various fields in thick brane. The dynamics and the final state of such long-lived modes are still unclear. In the thin brane, scattering of KK gravitons in the Randall–Sundrum II model has been considered [56,57]. It was proved that the brane possesses a set of discrete quasi-normal modes that appear as scattering resonance, and the graviton KK modes have a very short lifetime

Qin Tan and Yu-Peng Zhang are co-first authors of the article.

[a] e-mail: liuyx@lzu.edu.cn (corresponding author)

on the brane. Can KK modes exist in a thick brane for a long period like the long-lived resonance modes around a black hole? To answer this question, we take the scalar field as a simple example to study the evolution of scalar KK modes numerically. We will show the evolution behaviors of the scalar KK modes and obtain their half-life time on a brane. We will further analyze the feasibility of the KK resonances as a dark matter candidate. Although our research is still crude, it provides a stepping stone to further investigation of KK resonances of various fields on a thick brane.

The layout of the remaining part of this paper is as follows. In Sect. 2, we construct a thick brane solution in five-dimensional spacetime as the background of a test scalar field evolution. In Sect. 3, the scalar field is evolved with the maximally dissipative boundary condition. Both resonances and nonresonances are used as initial data, and their evolution behaviors are compared. Finally, the conclusions and discussion are presented in Sect. 4.

2 Braneworld model in general relativity

Firstly, we consider the thick brane in five-dimensional spacetime. For the simplest case of general relativity with a canonical scalar field, the action is given by [23,24,36]

$$S=\int \mathrm{d}^5x\sqrt{-g}\left(\frac{1}{2\kappa_5^2}R-\frac{1}{2}g^{MN}\partial_M\phi\partial_N\phi-V(\phi)\right), \quad (1)$$

where κ_5 is the five-dimensional gravitational constant. We set $\kappa_5 = 1$ in this paper for convenience. The five-dimensional metric for our thick brane model is given by

$$\mathrm{d}s^2=\mathrm{e}^{2A(y)}\gamma_{\mu\nu}\mathrm{d}x^\mu\mathrm{d}x^\nu+\mathrm{d}y^2, \quad (2)$$

where $\mathrm{e}^{2A(y)}$ is the warp factor and $\gamma_{\mu\nu}$ is the induced metric on the brane with four-dimensional Poincareé invariance:

$$\gamma_{\mu\nu}\mathrm{d}x^\mu\mathrm{d}x^\nu=\begin{cases}\eta_{\mu\nu}\mathrm{d}x^\mu\mathrm{d}x^\nu,\\ -\mathrm{d}t^2+\mathrm{e}^{2kt}(\mathrm{d}x_1^2+\mathrm{d}x_2^2+\mathrm{d}x_3^2),\\ \mathrm{e}^{2kx_3}(-\mathrm{d}t^2+\mathrm{d}x_1^2+\mathrm{d}x_2^2)+\mathrm{d}x_3^2.\end{cases} \quad (3)$$

The above three cases correspond to the flat brane, de Sitter brane, and anti-de Sitter brane, respectively. Here, $\eta_{\mu\nu} = \mathrm{diag}(-1, 1, 1, 1)$ is the four-dimensional Minkowski metric, capital Latin letters $M, N, \ldots = 0, 1, 2, 3, 4$ denote the five-dimensional indices, and Greek letters $\mu, \nu, \ldots = 0, 1, 2, 3$ denote the four-dimensional indices. In this paper, we only consider the flat brane, i.e.,

$$\mathrm{d}s^2=\mathrm{e}^{2A(y)}\eta_{\mu\nu}\mathrm{d}x^\mu\mathrm{d}x^\nu+\mathrm{d}y^2. \quad (4)$$

The dynamical field equations are

$$R_{MN}-\frac{1}{2}Rg_{MN}=T_{MN}, \quad (5)$$

$$g^{MN}\nabla_M\nabla_N\phi=\frac{\partial V(\phi)}{\partial\phi}. \quad (6)$$

By substituting the metric (4) into Eqs. (5) and (6), we can obtain the explicit equations of motion

$$6A'^2+3A''=-V-\frac{1}{2}\phi'^2, \quad (7)$$

$$6A'^2=\frac{1}{2}\phi'^2-V, \quad (8)$$

$$\phi''+4A'\phi'=\frac{\partial V}{\partial\phi}, \quad (9)$$

where prime denotes the derivative with respect to the extra-dimensional coordinate y. Note that only two of the above equations are independent, but we must solve three functions: $A(y)$, $\phi(y)$, and $V(\phi)$. So we need to provide one of the three functions to solve these equations. Here, we provide the following warp factor:

$$A(y)=\ln\Big[\tanh\big(k(y+b)\big)-\tanh\big(k(y-b)\big)\Big], \quad (10)$$

where the parameter b has length dimension one and the parameter k has mass dimension one. This warp factor has been thoroughly investigated in previous literature [51,52,54]. It can be seen that the parameter b determines the thickness of the thick brane. In the next section, we will see that larger parameter b may result in more resonant KK modes. From Eqs. (7), (8), (9), and (10) we get the solution

$$\phi(y)=-i\sqrt{6}\,\mathrm{sech}(bk)\Big[\cosh(2bk)\mathrm{F}\big(iky;\tanh^2(bk)+1\big)-2\sinh^2(bk)\Pi\big(\mathrm{sech}^2(bk);iky;\tanh^2(bk)+1\big)\Big], \quad (11)$$

$$V(y)=\frac{3}{2}k^2\Big[-4\big(\tanh(k(y-b))+\tanh(k(b+y))\big)^2+\mathrm{sech}^2(k(y-b))+\mathrm{sech}^2(k(b+y))\Big], \quad (12)$$

where $\mathrm{F}(y, q)$ is the elliptic integral of the first kind and $\Pi(y, q, p)$ is the elliptic integral of the third kind. This solution was investigated in Ref. [54] in $f(T)$ gravity theory. The energy density for the above brane solution is

$$\rho=24k^2-6k^2\big(\tanh(k(y-b))+\tanh(k(b+y))\big)^2. \quad (13)$$

Plots of the above warp factor, scalar field, and energy density are shown in Fig. 1. Based on this braneworld background, we consider a test scalar field and study its evolution. We investigate its dynamic behavior numerically, and clarify whether their KK modes can exist on the brane for a long period.

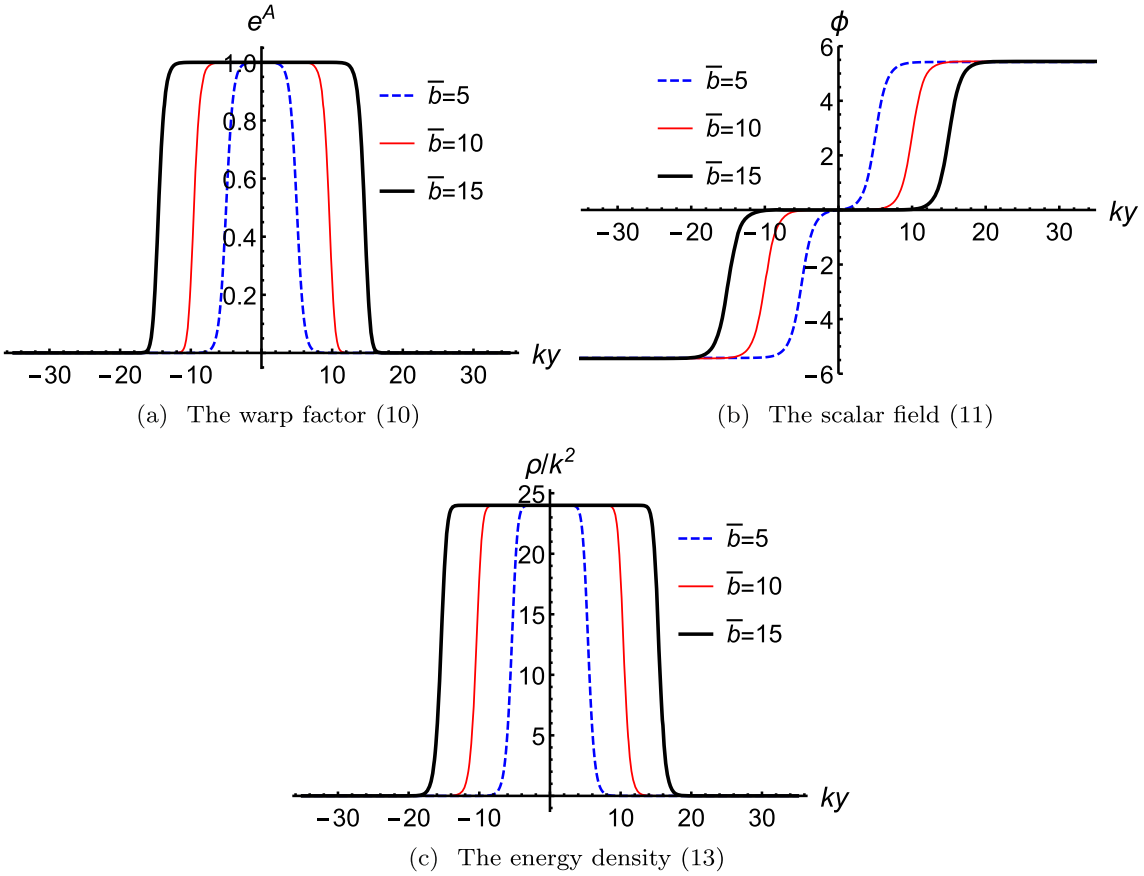

(a) The warp factor (10) (b) The scalar field (11)

(c) The energy density (13)

Fig. 1 The shapes of the warp factor (10), scalar field (11), and energy density (29)

3 Scalar field resonances and its evolution in braneworld

In this section we will consider the evolution of a scalar field in the thick brane given above. Here we consider a free massless test scalar field $\psi(x^M)$. Notice that the scalar field $\psi(x^M)$ here is not the background scalar field $\phi(y)$ that generates the thick brane. The equation of motion for the test field is the Klein–Gordon equation

$$\Box^{(5)}\psi = \frac{1}{\sqrt{-g}}\partial_M(\sqrt{-g}g^{MN}\partial_N\psi) = 0. \tag{14}$$

With the coordinate transformation $\mathrm{d}z = \mathrm{e}^{-A}\mathrm{d}y$, the metric (4) becomes a conformal flat one:

$$\mathrm{d}s^2 = \mathrm{e}^{2A(z)}(\eta_{\mu\nu}\mathrm{d}x^\mu\mathrm{d}x^\nu + \mathrm{d}z^2), \tag{15}$$

which is very useful in the derivation of the evolution equation and the Schrödinger-like equation of the test scalar field. In black hole physics, there is a similar coordinate, known as the tortoise coordinate. Then Eq. (14) can be written as

$$\left[\partial_z^2 + 3(\partial_z A)\partial_z + \eta^{\mu\nu}\partial_\mu\partial_\nu\right]\psi = 0. \tag{16}$$

We then introduce the following decomposition:

$$\psi(x^M) = \mathrm{e}^{-\frac{3}{2}A(z)}\Phi(t,z)\Xi(x^i). \tag{17}$$

Substituting the above decomposition (17) into Eq. (16), we get the following equation:

$$-\partial_t^2\Phi + \partial_z^2\Phi - U(z)\Phi - a^2\Phi = 0, \tag{18}$$

where a is a constant from the separation of variables. The effective potential $U(z)$ has the following form:

$$U(z) = \frac{3}{2}\partial_z^2 A + \frac{9}{4}(\partial_z A)^2, \tag{19}$$

or in the y coordinate equivalently

$$U(z(y)) = \frac{3}{2}\partial_y^2 A(y)\mathrm{e}^{2A(y)} + \frac{15}{4}\left(\partial_y A(y)\mathrm{e}^{A(y)}\right)^2. \tag{20}$$

The function $\Phi(t,z)$ can be further decomposed into oscillating modes as

$$\Phi(t,z) = \mathrm{e}^{i\omega t}u(z). \tag{21}$$

Substituting the above decomposition in Eq. (18) yields

$$-\partial_z^2 u(z) + U(z)u(z) = m^2 u(z), \tag{22}$$

where $m^2 = \omega^2 - a^2$ is the mass of the KK modes. We shall see below that the effective potential $U(z)$ is a volcano-like potential with a double-well. When $z \to \pm\infty$, $U(\pm\infty) \to 0_+$. Thus, all KK modes with $m^2 > 0$ are free states. Only the modes with $m^2 \leq 0$ could be bound states. One can show that there is no mode with $m^2 < 0$. The Schrödinger-like equation (22) can be factorized as the supersymmetric quantum mechanics form

$$\left(\partial_z + \frac{3}{2}\partial_z A(z)\right)\left(-\partial_z + \frac{3}{2}\partial_z A(z)\right)u(z) = m^2 u(z). \quad (23)$$

Using this supersymmetric quantum mechanics form with the conditions that $A(z)$ is a real function and the extra dimension z is noncompact, it can be shown that there is no tachyon mode with $m^2 < 0$ [58,59]. On the other hand, the solution of the zero mode with $m^2 = 0$ is

$$u_0(z) \propto \mathrm{e}^{\frac{3}{2}A(z)}. \quad (24)$$

Obviously, for the warp factor (10), the zero mode $u_0(z)$ is bound on the brane and it has no node along the extra dimension. According to the node theorem, the zero mode must be the ground state, which ensures that $m^2 \geq 0$. Solving Eq. (22), we get a series resonant modes, which can be treated as the initial data for the scalar field. The evolution is dominated by Eq. (18).

3.1 Scalar field resonances

In this part, we give a brief review on how to solve the KK scalar resonances. Substituting the warp factor (10) into Eq. (20), the effective potential in the coordinate y is [54]

$$\begin{aligned} U(z(y)) = &-\frac{3}{8}k^2\mathrm{sech}^2\big(k(b-y)\big)\mathrm{sech}^2\big(k(b+y)\big) \\ &\times\Big(\tanh\big(k(b-y)\big) + \tanh\big(k(b+y)\big)\Big)^2 \\ &\times\Big(-5\cosh(4ky) + 2\cosh\big(2k(b-y)\big) \\ &+ 2\cosh\big(2k(b+y)\big) + 9\Big). \end{aligned} \quad (25)$$

Plots of the above effective potential are shown in Fig. 2a. For convenience, we define the dimensionless parameters $\bar{b} = kb$ and $\bar{m} = m/k$. We can see that the width of the effective potential increases with $\bar{b}$. The resonant modes can be studied by the relative probability method which was proposed in Ref. [45]. The relative probability is defined as

$$P(m^2) = \frac{\int_{-z_b}^{z_b} |u(z)|^2 \mathrm{d}z}{\int_{-z_{\max}}^{z_{\max}} |u(z)|^2 \mathrm{d}z}, \quad (26)$$

where $u(z)$ is solved from Eq. (22), z_b is approximately the width of the brane, and $z_{\max}$ is a much larger width than z_b, and usually set to $10z_b$. If the relative probability has a peak with full width at half maximum around $m = m_n$, then there is a resonance with mass m_n. In this way, the modes whose amplitudes in the quasi-well are much larger than those outside the quasi-well can be found. These modes will remain on the brane for a longer time. Note that the wave functions can be even or odd because the potential is symmetric. Hence, the following boundary conditions can be used to solve Eq. (22) numerically:

$$u_{\mathrm{even}}(0) = 1, \quad \partial_z u_{\mathrm{even}}(0) = 0; \quad (27a)$$

$$u_{\mathrm{odd}}(0) = 0, \quad \partial_z u_{\mathrm{odd}}(0) = 1, \quad (27b)$$

where u_{even} denotes the even modes of $u(z)$ and u_{odd} denotes odd modes of $u(z)$. Substituting the effective potential (25) into the Schrödinger-like equation (22), we can obtain the solution of $u(z)$ numerically for a given mass m. Then the relative probability $P(m^2)$ can be obtained. The relative probability $P(m^2)$ of scalar resonances for $\bar{b} = 5$, 10, 15 are shown in Fig. 2a–c, respectively. The specific parameters of these resonances are listed in Table 1. It can be seen that the number of scalar resonances and their peak values increase with $\bar{b}$. Usually, the larger peak value means smaller full width at half maximum, and longer lifetime. We will see that in the next subsection.

3.2 Evolution of the scalar field resonances

Treating the scalar resonances as the initial data, we can evolve the scalar field under the evolution equation (18). Through the numerical evolution of the scalar field, we can obtain its lifetime on the brane. In this paper, we only consider the case of $a^2 = 0$, which means that scalar KK particles travel along the extra dimension at the speed of light at infinity. We also impose the maximally dissipative boundary condition, $\partial_n \Phi = \partial_t \Phi$ [60], where n is the outward unit normal vector to the boundary. Equation (18) is solved numerically using fourth-order finite differences in space, and evolving in time using a method of lines with a third-order Runge–Kutta integrator.

In order to more intuitively display the evolution of the scalar field, we define the conserved energy of the scalar field [61]

$$E = \int_{-\infty}^{\infty} \rho_E \mathrm{d}z, \quad (28)$$

where

$$\rho_E = \frac{1}{2}\left((\partial_t \Phi)^2 + \left(-\frac{3}{2}\partial_z A(z)\Phi + \partial_z \Phi\right)^2\right). \quad (29)$$

Firstly, we consider the evolution of resonances whose parameters are given in Table 1. We integrate the energy density ρ_E over $[-z_{\max}, z_{\max}]$, and the resulting energy will decay due to energy losses through both left and right boundaries. We plot the evolution of the integrated scalar field

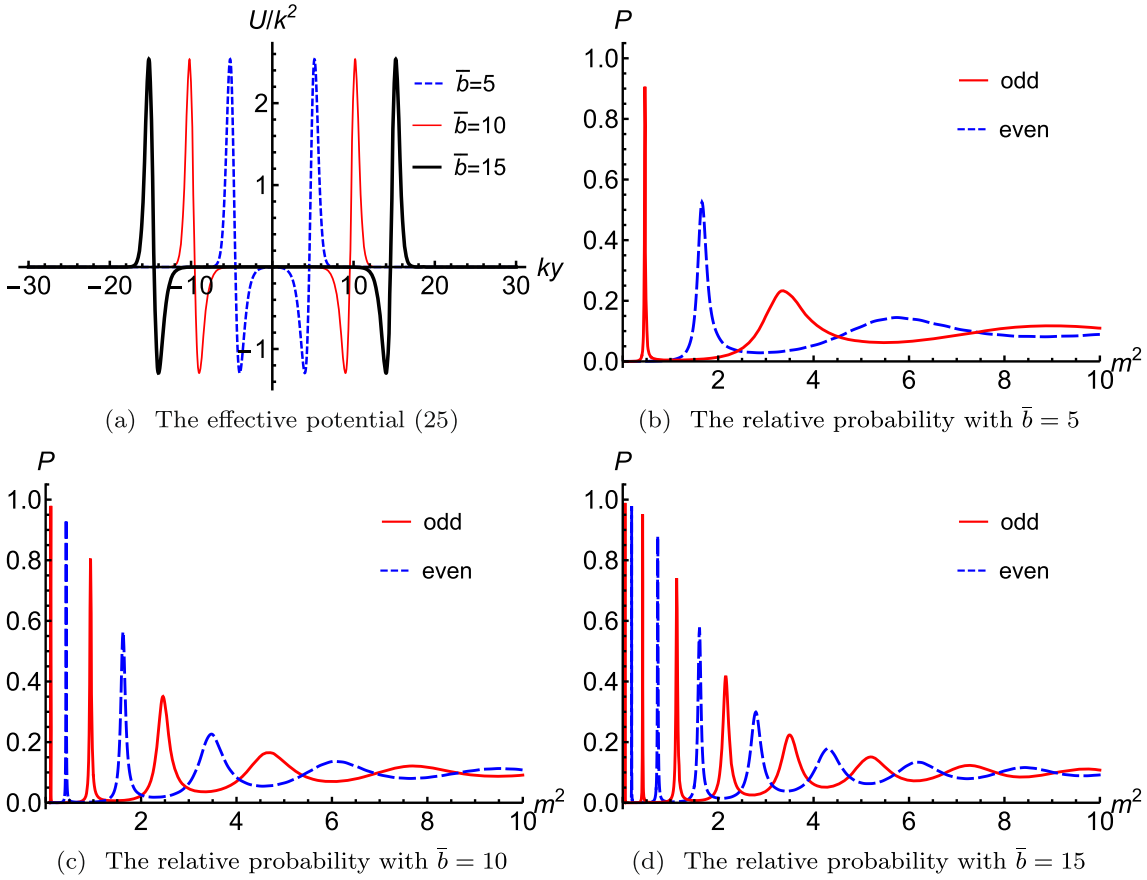

(a) The effective potential (25)

(b) The relative probability with $\bar{b} = 5$

(c) The relative probability with $\bar{b} = 10$

(d) The relative probability with $\bar{b} = 15$

Fig. 2 The shapes of the effective potential (25) for different parameters $\bar{b}$. The influence of the parameter $\bar{b}$ on the relative probability P for the odd-parity (red lines) and even-parity (blue dashed lines) massive KK modes. These figures are from Ref. [54]

energy $E(t)$ in Fig. 3. Note that it is plotted on a logarithmic scale. From Fig. 2b–d we can see that there are usually several resonances. Among these resonances, the first one will evolve the longest time. In addition, the evolution time increases with the parameter $\bar{b}$. This is because the larger $\bar{b}$, the more energy of the scalar field is concentrated in the potential well. In addition, we plot half-life time of the first resonance with different values of the parameter $\bar{b}$, which can be seen from Fig. 3d. Note that here we have defined the dimensionless time $\bar{t} = kt$. It can be clearly seen that the half-life time of the resonances increases with the parameter $\bar{b}$.

The energy decay can be fitted as an exponential function:

$$E(t) = E_0 \exp(-s\bar{t}), \tag{30}$$

where s is the fitting parameter and E_0 denotes the initial energy of the KK mode. Some results of the fit are listed in Table 2. It can be seen that both the scaled mass $\bar{m}_1$ and the fitting parameter s of the first resonance decrease with $\bar{b}$.

To better show the evolution of the scalar field over time, we analyze the result of the numerical evolution by extracting a time series for the resonance amplitude at a fixed point

Table 1 Resonant mass spectrum $\bar{m}_n^2$, $\bar{m}_n$, and relative probability P for different values of the parameter $\bar{b}$

$\bar{b}$	Parity	$\bar{m}_n^2$	$\bar{m}_n$	P
5	Odd	0.4649	0.6818	0.9064
	Even	1.6609	1.2888	0.5253
10	Odd	0.1088	0.3298	0.9794
	Even	0.4284	0.6545	0.9408
	Odd	0.9406	0.9698	0.8058
	Even	1.6216	1.2734	0.5648
	Odd	2.4585	1.5680	0.3508
15	Odd	0.0469	0.2165	0.9892
	Even	0.1866	0.4320	0.9803
	Odd	0.4169	0.6457	0.9516
	Even	0.7337	0.8566	0.8819
	Odd	1.1323	1.0641	0.7523
	Even	1.6078	1.2680	0.5796
	Odd	2.1585	1.4692	0.4193
	Even	2.7892	1.6701	0.2992

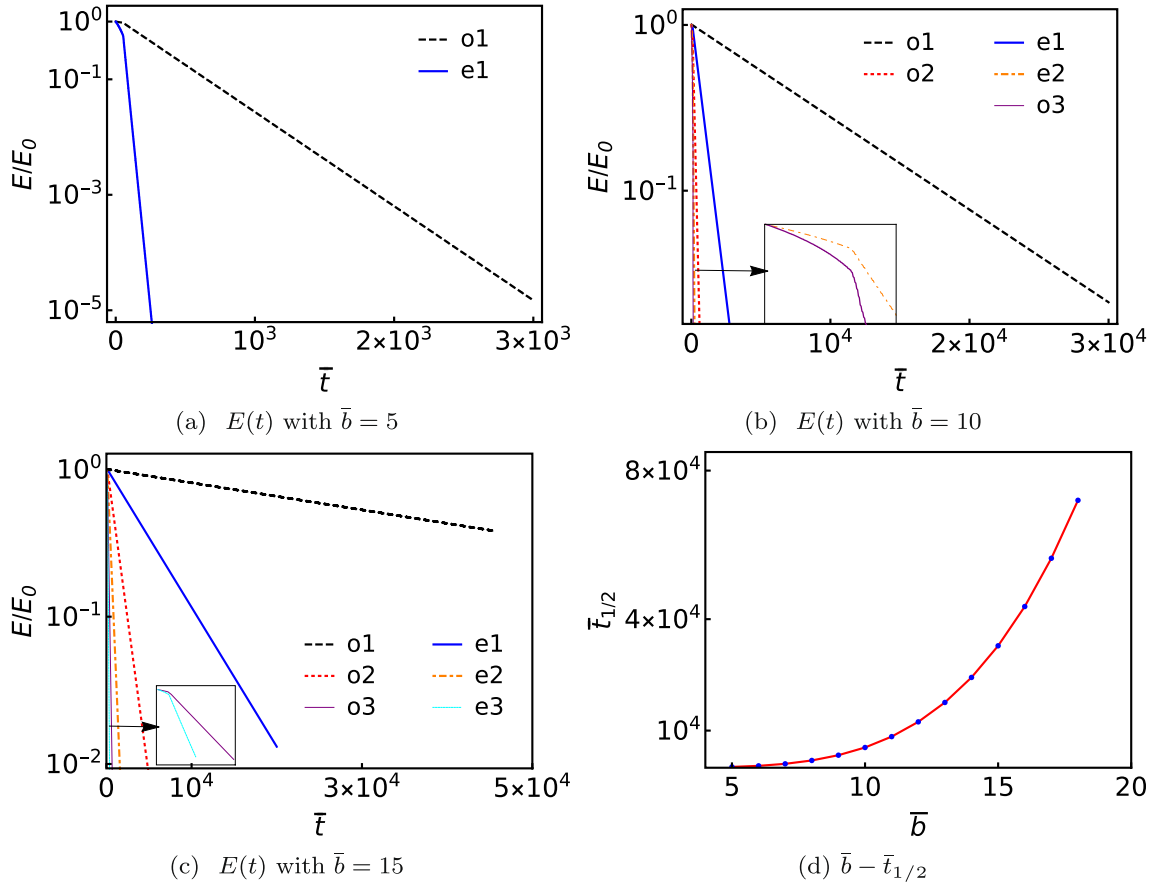

(a) $E(t)$ with $\bar{b} = 5$ (b) $E(t)$ with $\bar{b} = 10$

(c) $E(t)$ with $\bar{b} = 15$ (d) $\bar{b} - \bar{t}_{1/2}$

Fig. 3 **a–c** The energy of the scalar field vs. time for the evolution of the resonant modes for different values of the parameter $\bar{b}$. Here, o1 represents the first odd-parity resonance, e1 represents the first even-parity resonance, and so on. **d** The relation between the half-life of the first scalar resonance and the parameter $\bar{b}$

Table 2 The first resonant mass spectrum $\bar{m}_1^2$, $\bar{m}_1$, fitting parameter s, and half-life $t_{1/2}$ for different values of the parameter $\bar{b}$

$\bar{b}$	$\bar{m}_1^2$	$\bar{m}_1$	s	$t_{1/2}$ (if $k = 10^{-10}$ eV)
5	0.4649	0.6818	3.7527×10^{-3}	1.1969×10^{-3} s
6	0.3177	0.5636	1.4624×10^{-3}	3.0714×10^{-3} s
7	0.2298	0.4794	6.9109×10^{-4}	6.4993×10^{-3} s
8	0.1736	0.4166	3.6373×10^{-4}	1.2349×10^{-2} s
9	0.1356	0.3682	2.0910×10^{-4}	2.1481×10^{-2} s
10	0.1088	0.3298	1.2867×10^{-4}	3.4908×10^{-2} s
11	0.0892	0.2986	8.3435×10^{-5}	5.3833×10^{-2} s
12	0.0744	0.2728	5.6502×10^{-5}	7.9494×10^{-2} s
13	0.0630	0.2510	3.9624×10^{-5}	1.1334×10^{-1} s
14	0.0540	0.2324	2.8609×10^{-5}	1.5700×10^{-1} s
15	0.0469	0.2165	2.1170×10^{-5}	2.1217×10^{-1} s
16	0.0410	0.2026	1.6000×10^{-5}	2.8072×10^{-2} s
17	0.0362	0.1903	1.2316×10^{-5}	3.6470×10^{-1} s
18	0.0322	0.1794	9.6335×10^{-6}	4.6625×10^{-1} s

z_{ext}. The results are shown in Fig. 4. It can be seen that the resonance amplitude decreases with evolutionary time, and the amplitude attenuation of the second resonance is significantly faster than that of the first resonance. This also shows that the first resonance will evolve the longest. By comparing the amplitude attenuation at different positions of the same resonance, it can be seen that the attenuation rate and the overall shape are basically the same. In other words, at least for the first two resonances, there is no beating effect found in Ref. [62] for a black hole system.

As a comparison, we also consider the evolution of the nonresonances. These results are shown in Fig. 5. We find that the energy and amplitude of nonresonance decay very fast at the early stage, but later they decay like those of resonances. In order to gain a better understanding of the above results, we perform a spectral analysis. We calculate the discrete Fourier transform in time of the scalar field at a fixed point $z = z_j$. The explicit expression of the discrete Fourier transform is

$$F[\Phi(t)](f) := \left| A \sum_p \Phi(t_p, z_j) \exp(-2\pi i f t_p) \right|, \qquad (31)$$

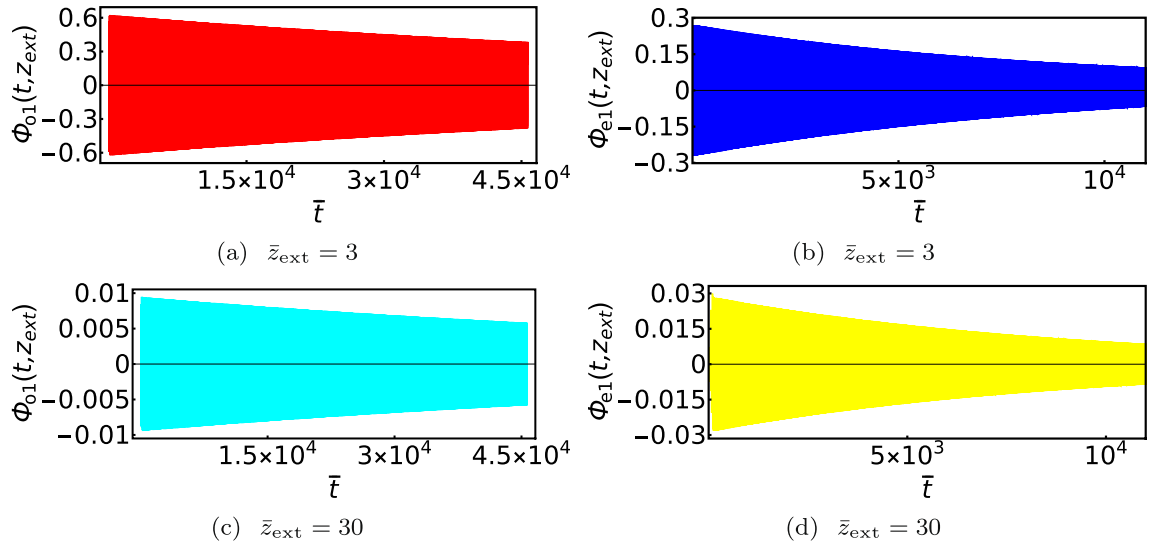

(a) $\bar{z}_{\rm ext} = 3$ (b) $\bar{z}_{\rm ext} = 3$

(c) $\bar{z}_{\rm ext} = 30$ (d) $\bar{z}_{\rm ext} = 30$

Fig. 4 Upper panel: Time evolution of the first odd resonance (left) and the first even resonance (right) at $\bar{z}_{\rm ext} = 3$ for $\bar{b} = 15$. Lower panel: Time evolution of the first odd resonance (left) and the first even resonance (right) at $\bar{z}_{\rm ext} = 30$ for $\bar{b} = 15$. Here $\bar{z}_{\rm ext} = kz_{\rm ext}$

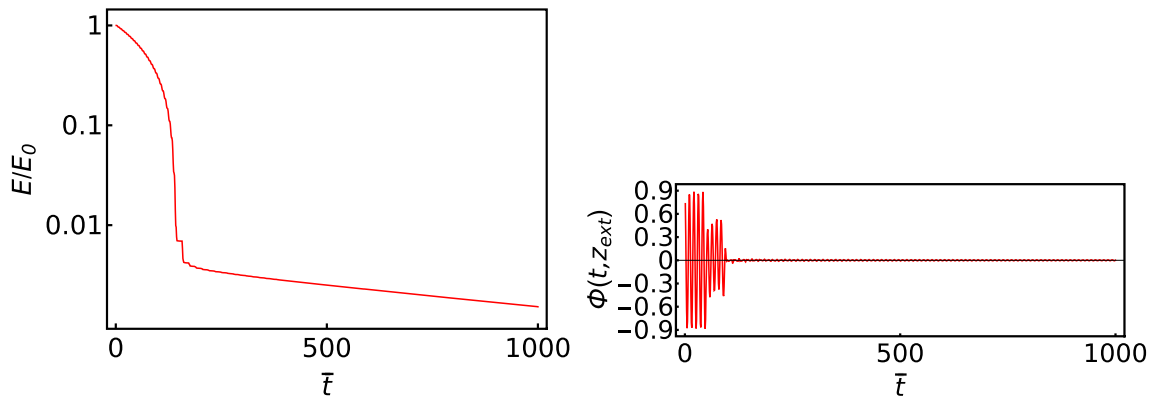

(a) $\bar{z}_{\rm ext} = 3$ (b) $\bar{z}_{\rm ext} = 30$

Fig. 5 Left panel: The energy of the scalar field vs. time for the evolution of nonresonance for $\bar{b} = 15$. Right panel: Time evolution of the nonresonance with $\bar{z}_{\rm ext} = 30$ for $\bar{b} = 15$

where A is normalization constant and t_p are the discrete time values. Plots of the Fourier transform for the first resonance and the nonresonance with $\bar{m}^2 = 0.36$ for $\bar{b} = 15$ are shown in Fig. 6. We find that for the Fourier transform of the resonance, there is only one peak corresponding to the resonance frequency. However, for the Fourier transform of the nonresonance, there are several peaks. Thus, nonresonances can evolve into combinations of resonances, and from this point of view, resonances seem to play a similar role in the braneworld as the quasi-normal modes in black holes physics, which deserves further investigation.

Finally, we consider the half-life time of the scalar resonances. If the exponential decay (30) is sustained throughout all evolution, then it is easy to determine that $\bar{t}_{1/2} = \frac{\ln(2)}{s}$. For $k = 10^{-10}$eV and $s = 10^{-10}$, the half-life time $t_{1/2}$ of the first scalar resonance will reach 10^4 seconds. Admittedly, it is still short compared with the age of our universe. But note that the lifetime of resonances increases with the parameter $\bar{b}$. Thus, for a very large $\bar{b}$, the lifetime of resonance might reach the cosmological time scale. Here, we can simply estimate the feasibility of resonance as a candidate for dark matter. For the braneworld model in this part, the effective four-dimensional Planck scale $M_{\rm Pl}$ and the fundamental five-dimensional scale M_5 have the relation

$$M_{\rm Pl}^2 = \frac{8\bar{b}\coth(2\bar{b}) - 4}{k} M_5^3. \tag{32}$$

According to the current experiment of the Large Hadron Collider, the collision energy is 13 TeV, but no signal of extra dimensions is seen [63], so the fundamental five-dimensional scale M_5 should be greater than 13 TeV. Thus, combining

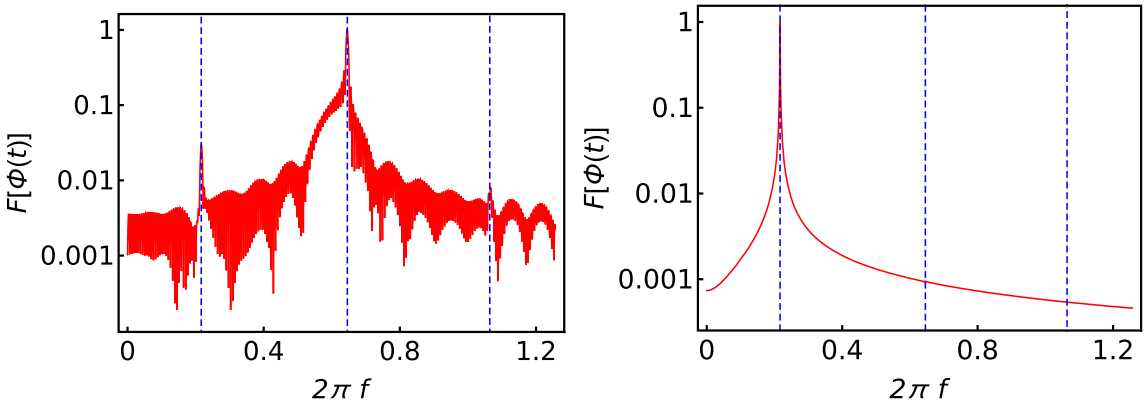

(a) $\bar{z}_{\rm ext} = 3$ (b) $\bar{z}_{\rm ext} = 3$

Fig. 6 Left panel: Discrete Fourier transform in time vs. frequency for the evolution of the nonresonance with $\bar{m}^2 = 0.36$ for $\bar{b} = 15$. Right panel: Discrete Fourier transform in time vs. frequency for the evolution of the first resonance with $\bar{m}_1^2 = 0.04687$ for $\bar{b} = 15$. The blue dotted lines correspond to the frequencies of the first three odd parity resonances

Eq. (32) and the condition $M_5 \gtrsim 13$ TeV, the constraint on the parameter k is given by

$$k \gtrsim (12\bar{b}\coth(2\bar{b}) - 6) \times 10^{-17}\ \text{eV}. \tag{33}$$

From Table 2, we can see that the fitting parameter s rapidly decreases with $\bar{b}$. In fact, when $\bar{b}$ doubles, the fitting parameter s decreases by an order of magnitude. If we choose $\bar{b} = 10^8$, then $k \geq 10^{-8}$ eV and s might be 10^{-25}, and the half-life time $t_{1/2}$ of the first scalar resonance will reach 10^{17} s, which is the same order of magnitude as the age of our universe (4.35×10^{17} s). On the other hand, the large $\bar{b}$ means that the first resonance is very light, but they are still hard to spot in the collider. This is because the cross section of any process involving the interaction of the zero mode with the light continuum modes is imperceptibly low. From this perspective, these long-lived resonances with very light mass could be considered as a candidate for dark matter.

4 Conclusion and discussion

In this paper, we numerically investigated the evolution of a free massless scalar field in the thick brane. We find that the resonances decay very slowly compared to the nonresonances and can exist on the brane for a very long period. If the lifetime of these resonances can be as long as the cosmological time scale, they might be a candidate for dark matter. This provides a new idea for dark matter research.

Firstly, we constructed a five-dimensional thick brane generated by a scalar field. Then, we considered the evolution of a test scalar field in this thick brane background. Through the coordinate transformation and the variable separation, we obtained the evolution equation (18) and the Schrödinger-like equation (22) for the extra-dimensional profile of the scalar field. The latter gives us the initial data of the massive KK modes, and the former evolves those initial data. Next we solved the Schrödinger-like equation (22) numerically to obtain the initial data of massive KK modes, in particular the initial data of the resonances. The results were shown in Fig. 2 and Table 1. We found that the relative probability of the first scalar resonance increases with $\bar{b}$, while the mass m_1 of the first scalar resonance decreases with $\bar{b}$. Using these KK modes as initial data, we investigated their evolution. Considering their energy decay and extracting a time series for the resonance amplitude, the evolution of the scalar field was analyzed. The results were shown in Figs. 3 and 4, and Table 2. The energy decay can be described by a decay parameter s which can be obtained by an exponential fit of E/E_0 as the function of $\bar{t}$. On the other hand, we also considered the evolution of the nonresonances. The energies and amplitudes of nonresonances decay rapidly at the early stage, but later they decay like those of the resonances. The behavior of the nonresonance evolution could be treated as a combination of resonances. Finally, we considered the half-life time of the resonance. For a very large $\bar{b}$, the lifetime of ultralight resonances can reach the cosmological time scale. These indicate that the scalar resonant mode could be a candidate for dark matter.

There is much to be improved in this paper. Firstly, the mass and interaction of the test scalar field is not taken into account, which might result in more interesting results. Secondly, other test fields such as Dirac spinor fields and gauge fields and their evolution are also worth investigating. These possibilities deserve further study.

Acknowledgements We are thankful to X.-L. Du, X.-H. Zhang, and J.-J. Wan for useful discussions. This work was supported by the National Key Research and Development Program of China (Grant no. 2020YFC2201503), the National Natural Science Foundation of China (Grants no. 11875151, no. 11705070, no. 12105126, and no. 12047501), the 111 Project under Grant no. B20063, the Fundamental Research

Funds for the Central Universities (Grant no. lzujbky2021-pd08), the China Postdoctoral Science Foundation (Grants no. 2021M701529 and 2021M701531), and "Lanzhou City's scientific research funding subsidy to Lanzhou University".

Data Availability Statement This manuscript has no associated data or the data will not be deposited. [Authors' comment: Our data is presented in the form of formulas and pictures, which are enough to explain our results. There is no need to list specific data.]

Funded by SCOAP[3]. SCOAP[3] supports the goals of the International Year of Basic Sciences for Sustainable Development.

References

1. N. Aghanim et al. (Planck), Planck 2018 results. VI. Cosmological parameters. Astron. Astrophys. **641**, A6 (2020). arXiv:1807.06209. [Erratum: Astron. Astrophys. **652**, C4 (2021)]
2. J. Barranco, A. Bernal, J.C. Degollado, A. Diez-Tejedor, M. Megevand, M. Alcubierre, D. Nunez, O. Sarbach, Are black holes a serious threat to scalar field dark matter models? Phys. Rev. D **84**, 083008 (2011). arXiv:1108.0931
3. J. Barranco, A. Bernal, J.C. Degollado, A. Diez-Tejedor, M. Megevand, M. Alcubierre, D. Nunez, O. Sarbach, Schwarzschild black holes can wear scalar wigs. Phys. Rev. Lett. **109**, 081102 (2012). arXiv:1207.2153
4. J. Barranco, A. Bernal, J.C. Degollado, A. Diez-Tejedor, M. Megevand, M. Alcubierre, D. Núñez, O. Sarbach, Schwarzschild scalar wigs: spectral analysis and late time behavior. Phys. Rev. D **89**, 083006 (2014). arXiv:1312.5808
5. X.N. Zhou, X.L. Du, K. Yang, Y.X. Liu, Dirac dynamical resonance states around Schwarzschild black holes. Phys. Rev. D **89**, 043006 (2014). arXiv:1308.2863
6. G.H. Gossel, J.C. Berengut, V.V. Flambaum, Resonance scattering and the passage to bound states in the field of near-black-hole objects. Int. J. Mod. Phys. D **23**, 1450089 (2014). arXiv:1308.6426
7. Y. Décanini, A. Folacci, M. Ould El Hadj, Resonant excitation of black holes by massive bosonic fields and giant ringings. Phys. Rev. D **89**, 084066 (2014). arXiv:1402.2481
8. M.O.P. Sampaio, C. Herdeiro, M. Wang, Marginal scalar and Proca clouds around Reissner–Nordström black holes. Phys. Rev. D **90**, 064004 (2014). arXiv:1406.3536
9. J.C. Degollado, C.A.R. Herdeiro, Wiggly tails: a gravitational wave signature of massive fields around black holes. Phys. Rev. D **90**, 065019 (2014). arXiv:1408.2589
10. N. Sanchis-Gual, J.C. Degollado, P.J. Montero, J.A. Font, Quasistationary solutions of self-gravitating scalar fields around black holes. Phys. Rev. D **91**, 043005 (2015). arXiv:1412.8304
11. N. Sanchis-Gual, J.C. Degollado, P.J. Montero, J.A. Font, V. Mewes, Quasistationary solutions of self-gravitating scalar fields around collapsing stars. Phys. Rev. D **92**, 083001 (2015). arXiv:1507.08437
12. N. Sanchis-Gual, J.C. Degollado, P. Izquierdo, J.A. Font, P.J. Montero, Quasistationary solutions of scalar fields around accreting black holes. Phys. Rev. D **94**, 043004 (2016). arXiv:1606.05146
13. J. Barranco, A. Bernal, J.C. Degollado, A. Diez-Tejedor, M. Megevand, D. Nunez, O. Sarbach, Self-gravitating black hole scalar wigs. Phys. Rev. D **96**, 024049 (2017). arXiv:1704.03450
14. Y. Huang, D.-J. Liu, X.-H. Zhai, X.-Z. Li, Massive charged Dirac fields around Reissner–Nordström black holes: quasibound states and long-lived modes. Phys. Rev. D **96**, 065002 (2017). arXiv:1708.04761
15. C.A. Sporea, Quasibound states of the Dirac field in Schwarzschild and Reissner–Nordström black hole backgrounds. Mod. Phys. Lett. A **34**, 1950323 (2019). arXiv:1905.05086
16. T. Kaluza, Zum unitätsproblem der physik Sitzungsber. Preuss. Akad. Wiss. Berlin (Math. Phys.) **27**, 966 (1921)
17. O. Klein, Quantum theory and five-dimensional theory of relativity. (in German and English). Z. Phys. **37**, 895 (1926)
18. N. Arkani-Hamed, S. Dimopoulos, G.R. Dvali, The hierarchy problem and new dimensions at a millimeter. Phys. Lett. B **429**, 263 (1998). arXiv:hep-ph/9803315
19. L. Randall, R. Sundrum, A large mass hierarchy from a small extra dimension. Phys. Rev. Lett. **83**, 3370 (1999). arXiv:hep-ph/9905221
20. I. Antoniadis, N. Arkani-Hamed, S. Dimopoulos, G.R. Dvali, New dimensions at a millimeter to a Fermi and superstrings at a TeV. Phys. Lett. B **436**, 257 (1998). arXiv:hep-ph/9804398
21. L. Randall, R. Sundrum, An alternative to compactification. Phys. Rev. Lett. **83**, 4690 (1999). arXiv:hep-th/9906064
22. W.D. Goldberger, M.B. Wise, Modulus stabilization with bulk fields. Phys. Rev. Lett. **83**, 4922 (1999). arXiv:hep-ph/9907447
23. M. Gremm, Four-dimensional gravity on a thick domain wall. Phys. Lett. B **478**, 434 (2000). arXiv:hep-th/9912060
24. O. DeWolfe, D.Z. Freedman, S.S. Gubser, A. Karch, Modeling the fifth dimension with scalars and gravity. Phys. Rev. D **62**, 046008 (2000). arXiv:hep-th/9909134
25. C. Csaki, J. Erlich, T.J. Hollowood, Y. Shirman, Universal aspects of gravity localized on thick branes. Nucl. Phys. B **581**, 309 (2000). arXiv:hep-th/0001033
26. D. Bazeia, A.R. Gomes, L. Losano, R. Menezes, Braneworld models of scalar fields with generalized dynamics. Phys. Lett. B **671**, 402 (2009). arXiv:0808.1815
27. C. Charmousis, R. Emparan, R. Gregory, Self-gravity of brane worlds: a new hierarchy twist. JHEP **05**, 026 (2001). arXiv:hep-th/0101198
28. O. Arias, R. Cardenas, I. Quiros, Thick brane worlds arising from pure geometry. Nucl. Phys. B **643**, 187 (2002). arXiv:hep-th/0202130
29. C. Barcelo, C. Germani, C.F. Sopuerta, Thin-shell limit of branes in the presence of Gauss-Bonnet interactions. Phys. Rev. D **68**, 104007 (2003). arXiv:gr-qc/0306072
30. D. Bazeia, A.R. Gomes, Bloch brane. JHEP **05**, 012 (2004). arXiv:hep-th/0403141
31. O. Castillo-Felisola, A. Melfo, N. Pantoja, A. Ramirez, Localizing gravity on exotic thick 3-branes. Phys. Rev. D **70**, 104029 (2004). arXiv:hep-th/0404083
32. N. Barbosa-Cendejas, A. Herrera-Aguilar, 4D gravity localized in non Z_2 symmetric thick branes. JHEP **10**, 101 (2005). arXiv:hep-th/0511050
33. P. Koerber, D. Lust, D. Tsimpis, Type IIA AdS_4 compactifications on cosets, interpolations and domain walls. JHEP **07**, 017 (2008). arXiv:0804.0614
34. N. Barbosa-Cendejas, A. Herrera-Aguilar, M.A. Reyes Santos, C. Schubert, Mass gap for gravity localized on Weyl thick branes. Phys. Rev. D **77**, 126013 (2008). arXiv:0709.3552

35. M.C. Johnson, M. Larfors, Field dynamics and tunneling in a flux landscape. Phys. Rev. D **78**, 083534 (2008). arXiv:0805.3705
36. A. Herrera-Aguilar, D. Malagon-Morejon, R.R. Mora-Luna, U. Nucamendi, Aspects of thick brane worlds: 4D gravity localization, smoothness, and mass gap. Mod. Phys. Lett. A **25**, 2089 (2010). arXiv:0910.0363
37. Y.-X. Liu, Y. Zhong, Z.-H. Zhao, H.-T. Li, Domain wall brane in squared curvature gravity. JHEP **06**, 135 (2011). arXiv:1104.3188
38. S. Kanno, J. Soda, Quasi-thick codimension 2 braneworld. JCAP **0407**, 002 (2004). arXiv:hep-th/0404207
39. A.E.R. Chumbes, J.M. Hoff da Silva, M.B. Hott, A model to localize gauge and tensor fields on thick branes. Phys. Rev. D **85**, 085003 (2012). arXiv:1108.3821
40. A.A. Andrianov, V.A. Andrianov, O.O. Novikov, Localization of scalar fields on self-gravitating thick branes. Phys. Part. Nucl. **44**, 190 (2013). arXiv:1210.3698
41. M. Kulaxizi, R. Rahman, Higher-spin modes in a domain-wall universe. JHEP **10**, 193 (2014). arXiv:1409.1942
42. A. de Souza Dutra, G. P. de Brito, J. M. Hoff da Silva, Method for obtaining thick brane models. Phys. Rev. D **91**, 086016 (2015). arXiv:1412.5543
43. S. Chakraborty, S. SenGupta, Kinematics of radion field: a possible source of dark matter. Eur. Phys. J. C **76**, 648 (2016). arXiv:1511.00646
44. A. Karam, A. Lykkas, K. Tamvakis, Frame-invariant approach to higher-dimensional scalar–tensor gravity. Phys. Rev. D **97**, 124036 (2018). arXiv:1803.04960
45. Y.-X. Liu, J. Yang, Z.-H. Zhao, C.-E. Fu, Y.-S. Duan, Fermion localization and resonances on a de Sitter thick brane. Phys. Rev. D **80**, 065019 (2009). arXiv:0904.1785
46. C.A.S. Almeida, M.M. Ferreira, A.R. Gomes, R. Casana, Fermion localization and resonances on two-field thick branes. Phys. Rev. D **79**, 125022 (2009). arXiv:0901.3543
47. W.T. Cruz, L.J.S. Sousa, R.V. Maluf, C.A.S. Almeida, Graviton resonances on two-field thick branes. Phys. Lett. B **730**, 314 (2014). arXiv:1310.4085
48. Z.-G. Xu, Y. Zhong, H. Yu, Y.-X. Liu, The structure of $f(R)$-brane model. Eur. Phys. J. C **75**, 368 (2015). arXiv:1405.6277
49. C. Csaki, J. Erlich, T.J. Hollowood, Quasilocalization of gravity by resonant modes. Phys. Rev. Lett. **84**, 5932 (2000). arXiv:hep-th/0002161
50. Y.-P. Zhang, Y.-Z. Du, W.-D. Guo, Y.-X. Liu, Resonance spectrum of a bulk fermion on branes. Phys. Rev. D **93**, 065042 (2016). arXiv:1601.05852
51. Y. Zhong, Y. Zhong, Y.-P. Zhang, Y.-X. Liu, Thick branes with inner structure in mimetic gravity. Eur. Phys. J. C **78**, 45 (2018). arXiv:1711.09413
52. W.-D. Guo, Y. Zhong, K. Yang, T.-T. Sui, Y.-X. Liu, Thick brane in mimetic $f(T)$ gravity. Phys. Lett. B **800**, 135099 (2020). arXiv:1805.05650
53. T.-T. Sui, W.-D. Guo, Q.-Y. Xie, Y.-X. Liu, Generalized geometrical coupling for vector field localization on thick brane in asymptotic anti-de Sitter spacetime. Phys. Rev. D **101**, 055031 (2020). arXiv:2001.02154
54. Q. Tan, W.-D. Guo, Y.-P. Zhang, Y.-X. Liu, Gravitational resonances on $f(T)$-branes. Eur. Phys. J. C **81**, 373 (2021). arXiv:2008.08440
55. J. Chen, W.-D. Guo, Y.-X. Liu, Thick branes with inner structure in mimetic f(R) gravity. Eur. Phys. J. C **81**, 709 (2021). arXiv:2011.03927
56. S.S. Seahra, Ringing the Randall–Sundrum braneworld: metastable gravity wave bound states. Phys. Rev. D **72**, 066002 (2005). arXiv:hep-th/0501175
57. S.S. Seahra, Metastable massive gravitons from an infinite extra dimension. Int. J. Mod. Phys. D **14**, 2279 (2005). arXiv:hep-th/0505196
58. K. Yang, Y.-X. Liu, B. Guo, X.-L. Du, Scalar perturbations of Eddington-inspired Born–Infeld braneworld. Phys. Rev. D **96**, 064039 (2017). arXiv:1706.04818
59. J.-J. Wan, Z.-Q. Cui, W.-B. Feng, Y.-X. Liu, Smooth braneworld in 6-dimensional asymptotically AdS spacetime. JHEP **05**, 017 (2021). arXiv:2010.05016
60. M. Megevand, I. Olabarrieta, L. Lehner, Scalar field confinement as a model for accreting systems. Class. Quantum Gravity **24**, 3235 (2007). arXiv:0705.0644
61. V. Pavlidou, K. Tassis, T.W. Baumgarte, S.L. Shapiro, Radiative falloff in neutron star spacetimes. Phys. Rev. D **62**, 084020 (2000). arXiv:gr-qc/0007019
62. H. Witek, V. Cardoso, A. Ishibashi, U. Sperhake, Superradiant instabilities in astrophysical systems. Phys. Rev. D **87**, 043513 (2013). arXiv:1212.0551
63. M. Aaboud et al. (ATLAS), Search for heavy ZZ resonances in the $\ell^+\ell^-\ell^+\ell^-$ and $\ell^+\ell^-\nu\bar{\nu}$ final states using proton–proton collisions at $\sqrt{s} = 13$ TeV with the ATLAS detector. Eur. Phys. J. C **78**, 293 (2018). arXiv:1712.06386